Propagating Wave Packets and Quantized Currents in Coherently Driven Polariton Superfluids

M. H. Szymańska,[1] F. M. Marchetti,[2] and D. Sanvitto[3,*]

[1]Department of Physics, University of Warwick, Coventry, CV4 7AL, United Kingdom
[2]Departamento de Física Teórica de la Materia Condensada, Universidad Autónoma de Madrid, Madrid 28049, Spain
[3]Departamento de Física de Materiales, Universidad Autónoma de Madrid, Madrid 28049, Spain

(Received 25 May 2010; revised manuscript received 16 August 2010; published 30 November 2010)

We study the properties of propagating polariton wave packets and their connection to the stability of doubly charged vortices. Wave-packet propagation and related photoluminescence spectra exhibit a rich behavior dependent on the excitation regime. We show that, because of the nonquadratic polariton dispersion, doubly charged vortices are stable only when initiated in wave packets propagating at small velocities. Vortices propagating at larger velocities, or those imprinted directly into the polariton optical parametric oscillator signal and idler, are unstable to splitting.

DOI: 10.1103/PhysRevLett.105.236402 PACS numbers: 71.36.+c, 42.65.Yj, 47.32.C−

A decade after the first reports of bosonic stimulation [1,2], resonantly pumped polaritons are shown to exhibit a new form of nonequilibrium superfluid behavior [3–5]. The experimental ability to control externally the polariton currents (phase variations) with a laser pump [4], as well as to generate propagating polariton wave packets (density and phase variations), by applying another pulsed laser probe [3], is a unique feature of driven polariton systems. Here, the interplay between phase and amplitude variations opens the possibility for novel superfluid phenomena. In addition, by using a pulsed Laguerre-Gauss beam, polaritons in the optical parametric oscillator (OPO) regime have recently been shown to display persistence of currents and metastability of quantum vortices with charges $m = 1$ and $m = 2$ [5].

In this Letter we report a comprehensive analysis of propagating polariton wave packets, triggered by a pulsed probe, and examine the stability of vortices of charge $m = 2$ in different excitation regimes. In particular, we assess how the wave-packet shape, velocity, and intensity, as well as the stability of $m = 2$ vortices, are related to the probe wave vector and to the photoluminescence (PL) spectra. The behavior of $m = 2$ vortices has been studied recently [5], and two distinct regimes have been singled out: In one regime the initiated vortex only lasts for as long as the additional decaying gain introduced by the triggering probe. Here, $m = 2$ vortices have been shown to be remarkably stable when initiated at small group velocities and instead to split into two $m = 1$ vortices at larger velocities. In a second regime, vortices withstand the gain and imprint into the OPO. In this case, $m = 2$ vortices always split. We provide the theoretical explanation for this intriguing phenomenon.

The behavior of $m = 2$ vortices has been the subject of intensive research in the context of ultracold atomic gases. However, although stable free $m = 2$ vortices have been predicted for specific ranges of density and interaction strength [6,7], they have not been observed experimentally [8]. Stable pinned $m = 2$ persistent currents have been realized [9] only by using toroidal traps.

Model.—The time evolution of coherently driven polaritons is described by the Gross-Pitaevskii equations for coupled cavity photon and exciton fields $\psi_{C,X}(\mathbf{r}, t)$ with pump and decay ($\hbar = 1$) [10]:

$$i\partial_t \begin{pmatrix} \psi_X \\ \psi_C \end{pmatrix} = \begin{pmatrix} 0 \\ F_p + F_{\mathrm{pb}} \end{pmatrix} + \begin{pmatrix} \omega_X - i\kappa_X + g_X|\psi_X|^2 & \Omega_R/2 \\ \Omega_R/2 & \omega_C - i\kappa_C \end{pmatrix} \times \begin{pmatrix} \psi_X \\ \psi_C \end{pmatrix}. \quad (1)$$

We use here the same notation as in Ref. [11]. The cavity field is driven by a continuous-wave pump, $F_p(\mathbf{r}, t) = \mathcal{F}_{f_p,\sigma_p}(r)e^{i(\mathbf{k}_p\cdot\mathbf{r}-\omega_p t)}$, with a Gaussian or a top-hat spatial profile $\mathcal{F}_{f_p,\sigma_p}$ of strength f_p and a FWHM of σ_p. $F_{\mathrm{pb}}(\mathbf{r}, t)$ is the pulsed probe introduced later. We neglect the exciton dispersion and assume a quadratic dispersion for photons, $\omega_C = \omega_C^0 - \frac{\nabla^2}{2m_C}$. Ω_R is the Rabi splitting, and the fields decay with rates $\kappa_{X,C}$. The exciton interaction strength g_X is set to 1 by rescaling both fields $\psi_{X,C}$ and pump strengths F_p and F_{pb} by $\sqrt{\Omega_R/(2g_X)}$. Throughout this Letter, $m_C = 2 \times 10^{-5} m_0$, the energy zero is set to $\omega_X = \omega_C^0$ (zero detuning), and $\Omega_R = 4.4$ meV. We numerically solve Eq. (1) on a 2D grid using a fifth-order adaptive-step Runge-Kutta algorithm.

In the absence of the probe ($F_{\mathrm{pb}} = 0$), polaritons are continuously injected into the pump state and, above the pump strength threshold for OPO, f_p^{th}, they undergo stimulated scattering into the signal and idler states [2] (see Fig. 1, left panels). We filter the signal, idler, and pump spatial profiles $|\psi_{C,X}^{s,i,p}(\mathbf{r}, t)|e^{i\phi_{C,X}^{s,i,p}(\mathbf{r},t)}$ in a cone around their associated momenta $\mathbf{k}_{s,i,p}$. The supercurrent $\nabla\phi_{C,X}^{s,i,p}$ is a

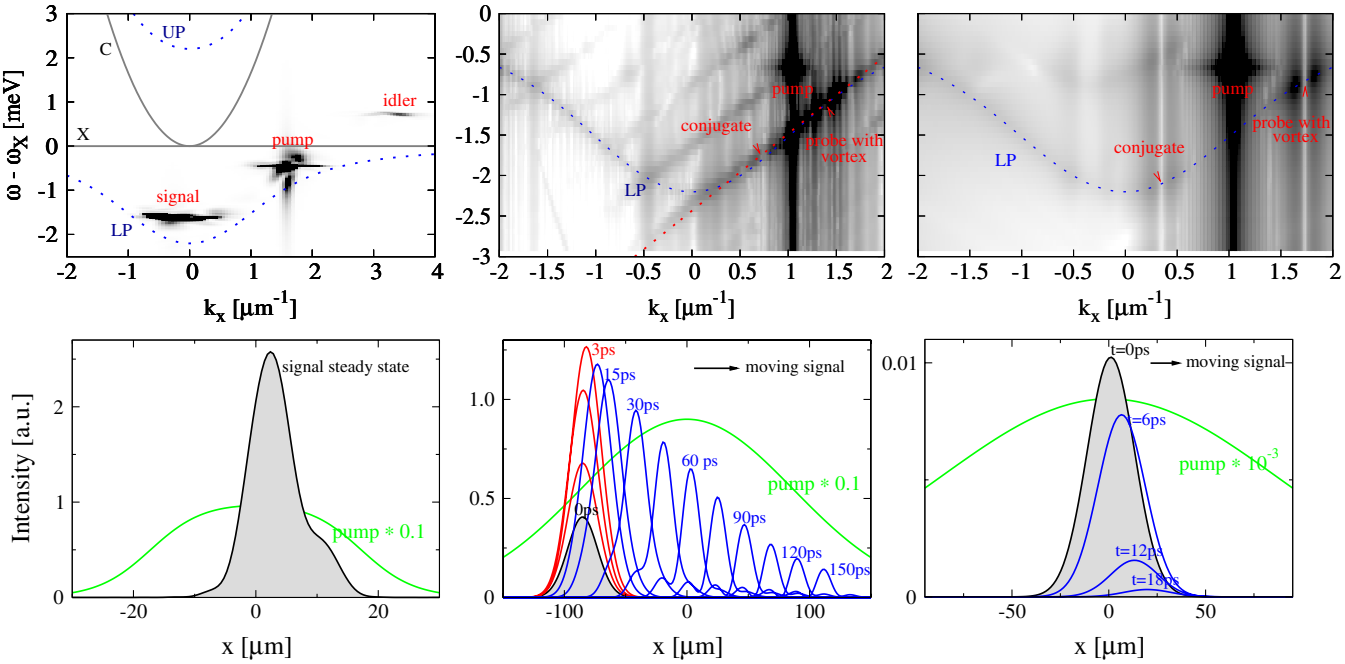

FIG. 1 (color online). PL spectra (top panels) and spatial profiles of pump and filtered signals $|\psi_C^s(x, 0, t)|$ (bottom panels) for three regimes: (i) OPO (left panels) for a smoothened top-hat pump above threshold ($f_p = 1.12 f_p^{(\mathrm{th})}$)—polaritons, continuously injected at $(k_p, 0)$ and ω_p, undergo stimulated scattering into signal and idler stationary steady states ($\kappa_{X,C} = 0.2$ meV). (ii) TOPO (middle panels): A short, $\sigma_t = 1$ ps, Laguerre-Gauss $m = 2$ (top panel) and Gaussian $m = 0$ (bottom panel) probe [Eq. (2)] resonant with $(k_{\mathrm{pb}}, 0)$ and ω_{pb} triggers propagating signal and conjugate states, which lock to the same group velocity ($\kappa_X = 0$, $\kappa_C = 0.02$ meV). (iii) Conditions similar to (ii) but $\kappa_{X,C} = 0.09$ meV (right panels); now there is no amplification of the probe, and both the signal and conjugate decay exponentially. LP and upper polariton (UP) (blue dashed lines), and bare cavity photon (C) and exciton (X) dispersions (gray dashed lines) are shown for reference.

superposition of the dominant uniform flow $\mathbf{k}_{s,i,p}$ and more complex currents (caused by the system being finite size), which move particles from gain to loss dominated regions. In addition, one can characterize the density variations defining the group velocity $\mathbf{v}_g^{s,i,p} = d\mathbf{r}_m^{s,i,p}/dt$, where $\mathbf{r}_m^{s,i,p}$ is the maximum of the signal (idler and pump) spatial profile. The OPO is a steady-state regime, where $|\psi_{C,X}^{s,i,p}(\mathbf{r}, t)|$ are time independent. This is also recognizable in the typical flat dispersion of signal, idler, and pump PL spectra (see left panel of Fig. 1)—the signal (idler, pump) group velocity being the derivative of the dispersion at $\mathbf{k}_s$ ($\mathbf{k}_{i,p}$).

Propagating wave packets and triggered OPO (TOPO) regime.—In order to create propagating wave packets (finite group velocity), one needs to add a pulsed probe with finite momentum $\mathbf{k}_{\mathrm{pb}}$, spatially small with respect to the pump spot size [3]. Since we are interested in the stability of triggered vortices of charge $m = 2$, and its connection to the character of the propagating wave packet, we consider here a Laguerre-Gauss pulsed probe [5,11,12],

$$F_{\mathrm{pb}}(\mathbf{r}, t) = f_{\mathrm{pb}}|\mathbf{r} - \mathbf{r}_{\mathrm{pb}}|^{|m|} e^{-|\mathbf{r}-\mathbf{r}_{\mathrm{pb}}|^2/(2\sigma_{\mathrm{pb}}^2)} e^{im\varphi} \times e^{i(\mathbf{k}_{\mathrm{pb}}\cdot\mathbf{r} - \omega_{\mathrm{pb}} t)} e^{-(t-t_{\mathrm{pb}})^2/(2\sigma_t^2)}, \quad (2)$$

where the phase φ winds from 0 to 2π around the vortex core $\mathbf{r}_{\mathrm{pb}}$. Above threshold for OPO, $f_p > f_p^{\mathrm{th}}$, one can identify two distinct regimes [5]: In one case, the triggered vortex propagates as extra population (gain) on top of the OPO stationary signal and idler states [3]—TOPO regime. Here, the vortex lasts only for as long as the additional decaying gain. A similar TOPO regime can be found also below the OPO threshold, and for simplicity, we show this case in Fig. 1 (middle panel). Alternatively, vortices persist the gain and imprint into the OPO signal and idler—metastable vortex regime [11].

In the TOPO regime, the polaritons generated by the probe scatter parametrically with the ones of the pump, generating a traveling signal (here meant as extra population on top of either the OPO signal or idler, or the full signal if below the OPO threshold) with momentum $\mathbf{k}_s = \mathbf{k}_{\mathrm{pb}}$ (which can be either $\mathbf{k}_{\mathrm{pb}} > \mathbf{k}_p$ or $\mathbf{k}_{\mathrm{pb}} < \mathbf{k}_p$) and its *conjugate* at $\mathbf{k}_c = 2\mathbf{k}_p - \mathbf{k}_{\mathrm{pb}}$. In the middle panels of Fig. 1 the signal and the conjugate initially get strongly amplified by the parametric scattering from the pump, then decay slowly, and, at later times, the decay becomes exponential. This regime reproduces the one observed in experiments (see Fig. 3 of Ref. [13]), where the intensity maximum is reached quickly, within 4 ps after the maximum of the pulsed probe, and is immediately followed by a slow decay. Instead, for the case of the right panels of Fig. 1, parametric scattering is too weak to induce any significant amplification, and we observe exponential decay of signal and conjugate populations immediately after

the probe switches off. By analyzing the change in time of the spatial profile of the TOPO signal $|\psi^s_{C,X}(\mathbf{r}, t)|$, we find that its group velocity v^s_g is simply given by the derivative of the lower polariton (LP) dispersion evaluated at $\mathbf{k}_{\rm pb}$, i.e., for zero detuning and low densities by $v^{\rm LP}_{k_{\rm pb}} \equiv k_{\rm pb}/(2m_C) - k^3/(2m_C\sqrt{k^4 + 4m_C^2\Omega_R^2})$ (see Fig. 2).

In order to understand this it is instructive to analyze the PL spectra. In the regime with weak parametric scattering (right panel of Fig. 1), aside the strong emission from the pump state, the dispersion is simply that of the LP, and thus the signal propagates with a group velocity given by $v^{\rm LP}_{k_{\rm pb}}$. However, in the TOPO regime (middle panel of Fig. 1) the spectrum is linear. This can be explained by the fact that, to have efficient parametric scattering, the signal and conjugate require a large spatial overlap and so their group velocities need to lock to the same value; therefore, the dispersion becomes linear—a similar result has been found in 1D simulations, as well as in experiments [3]. Here, we determine that the TOPO linear dispersion is tangential to the LP branch at $k_{\rm pb}$; thus, its slope is given, in this case, also by $v^{\rm LP}_{k_{\rm pb}}$.

The linearization of the TOPO dispersion, with the slope given by $k_{\rm pb}$, also explains our observation that the TOPO amplification is stronger when signal ($\mathbf{k}_s = \mathbf{k}_{\rm pb}$) and conjugate ($\mathbf{k}_c$) wave vectors have nearby values. This implies that the LP tangential line at $\mathbf{k}_{\rm pb}$ lies close to the LP dispersion also at $\mathbf{k}_c$, leading to efficient stimulation. It is interesting to note that by changing $\mathbf{k}_p$ and $\mathbf{k}_{\rm pb}$, it is possible to engineer wave packets with a broad range of values of group velocities and supercurrents—e.g., for $\mathbf{k}_{\rm pb} = 2\mathbf{k}_p$, one has a conjugate state at $\mathbf{k}_c = 0$ (i.e., no net current) with a large group velocity, $v^c_g = v^{\rm LP}_{2k_p}$.

From the PL spectrum we can deduce the nature of the wave-packet propagation. For linear dispersion one expects a solitonlike behavior, with the signal and conjugate propagating and not changing shape or intensity. For quadratic dispersion, propagation is analogous to the ballistic time-of-flight expansion of ultracold atomic gases [14]; i.e., for a Gaussian wave packet, the FWHM $= [\sigma^2_{\rm pb} + (\frac{t}{2m_C\sigma_{\rm pb}})^2]^{1/2}$ grows in time, but the shape is preserved. The total density decays exponentially with a rate given by $\frac{\kappa_C+\kappa_X}{2}$ at zero detuning, and the maximum of the wave packet moves with a constant velocity $v^{\rm LP}_{k_{\rm pb}}$ (equal to $\frac{\mathbf{k}_{\rm pb}}{2m_C}$ in the quadratic LP regime). Because of the dynamical nature of the TOPO state, the system evolves between different regimes. In particular, only in the strong amplification regime is the spectrum linear, while it evolves back to the LP at longer times. In addition, when the LP dispersion deviates from quadratic, propagation becomes complex: The wave packet gets distorted and one observes beatings in the spatial profiles.

Propagation of the signal and conjugate is shown in the right panel of Fig. 2. We observe a mechanism analogous to the one found in four-wave-mixing experiments [15,16]: When the probe arrives, the conjugate propagates faster than the signal, before getting locked to it with a small spatial shift of their maximum intensities. At later times, when the density drops and the parametric process becomes inefficient, the two wave packets start unlocking—the conjugate slows down with respect to the signal if $k_c < k_s$, as in Fig. 2, or moves faster when $k_c > k_s$.

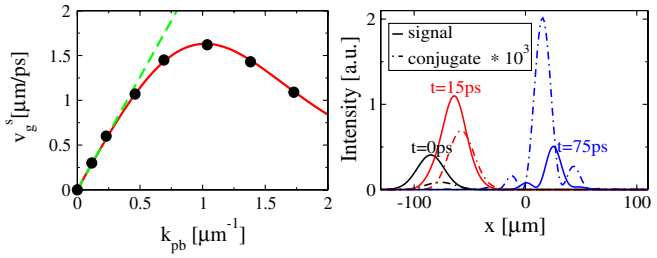

FIG. 2 (color online). Left panel: Group velocity v^s_g of the propagating signal wave packet versus the probe momentum $k_{\rm pb}$. The black dots are determined from simulations, whereas the solid line (red) is the derivative of the LP dispersion evaluated at $k_{\rm pb}$, $v^{\rm LP}_{k_{\rm pb}}$. The green dashed line indicates where the LP dispersion deviates from the quadratic. Right panel: Signal (solid lines) and conjugate (dashed lines) states for $k_{\rm pb} = 1.4\ \mu{\rm m}^{-1}$ at different times after the arrival of the probe.

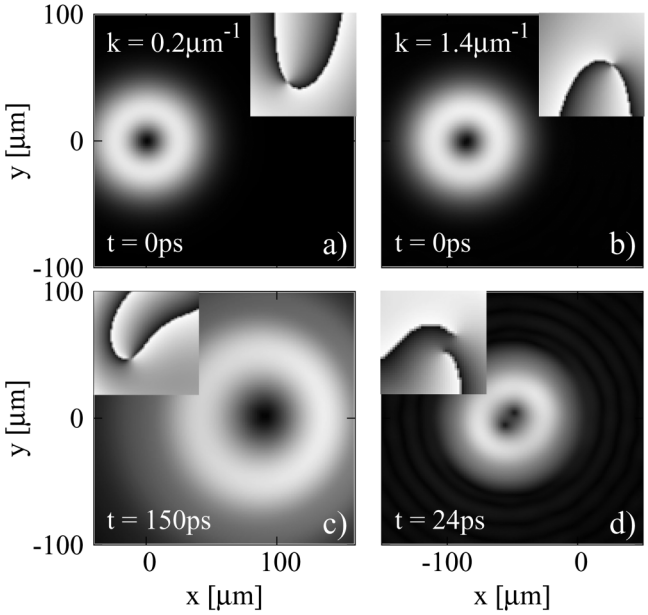

FIG. 3. Profiles of the TOPO signal intensity $|\psi^s_C(\mathbf{r}, t)|$ and phase $\phi^s_C(\mathbf{r}, t)$ (inset) after the arrival (at $t = 0$) of an $m = 2$ vortex pulsed probe [Eq. (2)] with $\sigma_{\rm pb} \simeq 87\ \mu$m. The conditions are the same as the middle panels of Fig. 1, but with $k_{\rm pb} = 0.2\ \mu{\rm m}^{-1}$ (a, c) and $k_{\rm pb} = 1.4\ \mu{\rm m}^{-1}$ (b, d). While in (a, c) the $m = 2$ vortex does not split within its lifetime, in (b, d) the vortex splits soon after the probe arrives. The intensity scale in (c) is 200 times smaller than in (a).

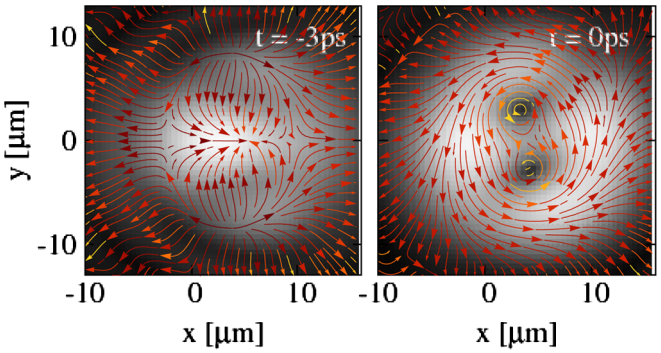

FIG. 4 (color online). Filtered signal profile and currents above OPO threshold $f_p = 1.12 f_p^{(\mathrm{th})}$ for a top-hat pump with FWHM $\sigma_p = 35\mu$m at $t = -3$ ps (left panel) before the arrival of an $m = 2$ probe at $t = 0$ ps (right panel). The double quantized vortex splits into two $m = 1$ vortices even before the probe reaches its maximum intensity.

Stability of $m = 2$ TOPO vortices.—In the TOPO regime, we observe $m = 2$ vortices to be stable within their lifetime when triggered at small momenta k_{pb} [Figs. 3(a) and 3(c)], while TOPO vortices always split into two $m = 1$ vortices for large k_{pb} [Figs. 3(b) and 3(d)], in agreement with the recent experimental observations [5]. Our numerical analysis shows that the crossover from nonsplitting to splitting happens for the probe momentum where the LP dispersion deviates from quadratic (see Fig. 2). The two regimes are shown in Fig. 3: For $k_{\mathrm{pb}} = 0.2\ \mu\mathrm{m}^{-1}$, at short times, the signal propagates without changing shape and with little change in intensity, consistent with a linear dispersion in the PL spectrum. However, at longer times the density drops more than 2 orders of magnitude, the dispersion becomes quadratic, and the wave packet expands (panel c). A uniform expansion of the wave packet leads to an increase of the vortex core but does not cause the vortex to split. In contrast, for $k_{\mathrm{pb}} = 1.4\ \mu\mathrm{m}^{-1}$, where the LP dispersion is not quadratic, the splitting of the $m = 2$ vortex state into two $m = 1$ vortices happens shortly after the arrival of the probe (panel d). This behavior can be explained as follows: The dispersion of the time-dependent TOPO evolves from the LP (before the probe arrival) to linear (at early times after the probe arrival), and back to the LP at later times. Wave packets propagating with nonquadratic dispersion do not keep their shapes. Indeed, we see that the distortion is very pronounced at later times of the evolution. This distortion during the propagation leads to the mechanical splitting of an $m = 2$ vortex, analogous to the structural instability discussed in [17]. Also, for small k_{pb}, within the quadratic part of the dispersion, the group velocity of the vortex and the velocity of the net supercurrent (given by k_{pb}) are equal. However, this is not the case for larger k_{pb}, beyond the quadratic part, and so the propagating vortex feels a rather strong net current in its frame, which may provide an additional explanation for splitting.

$m = 2$ vortices imprinted into the OPO.—As in Ref. [5], we find that an $m = 2$ vortex imprinted into the OPO signal is never stable, and splits into two $m = 1$ vortices almost immediately, even before the probe reaches its maximum intensity (see Fig. 4). There are several causes of the splitting: Before the probe arrives, the OPO dispersion is flat around the signal, idler, and pump. However, the triggering probe favors the signal and conjugate to lock and propagate with the same velocity $v^{\mathrm{LP}}_{k_{\mathrm{pb}}}$, which corresponds to a linear dispersion. Further, once the vortex gets imprinted into the stationary OPO signal and idler, the dispersion becomes flat again. The evolution of the dispersion between linear and flat leads to complicated dynamics of both the signal and the idler, causing the structural instability and splitting of the vortex during the transient time. Another reason for the structural instability is the nonuniform current (see Fig. 4) caused by the interplay between spatial inhomogeneity, pump and decay, which the OPO vortex experiences in its reference frame.

To conclude, we have determined group velocity and supercurrents of propagating polariton wave packets triggered by a pulsed laser probe, and established the conditions under which $m = 2$ vortices are stable and when they split into two vortices of $m = 1$. Both phenomena are related to the form of the PL spectrum and the wave vector of the triggering probe. The ability to control the topological charge and number of vortices, simply by changing the wave vector of the external probe, holds potential for operations in quantum information.

We thank E. Cancellieri, J. Keeling, C. Tejedor, and L. Viña for discussions; TCM, Cavendish Lab, Cambridge for the use of computer resources; and Ramón y Cajal, INTELBIOMAT (ESF), Spanish MEC QOIT-CSD2006-00019, and CAM S2009/ESP-1503 for financial support.

*Present address: Istituto Nanoscienze CNR, Lecce, Italy.

[1] P. G. Savvidis *et al.*, Phys. Rev. Lett. **84**, 1547 (2000).
[2] R. M. Stevenson *et al.*, Phys. Rev. Lett. **85**, 3680 (2000).
[3] A. Amo *et al.*, Nature (London) **457**, 291 (2009).
[4] A. Amo *et al.*, Nature Phys. **5**, 805 (2009).
[5] D. Sanvitto *et al.*, Nature Phys. **6**, 527 (2010).
[6] H. Pu *et al.*, Phys. Rev. A **59**, 1533 (1999).
[7] M. Möttönen *et al.*, Phys. Rev. A **68**, 023611 (2003).
[8] Y. Shin *et al.*, Phys. Rev. Lett. **93**, 160406 (2004).
[9] C. Ryu *et al.*, Phys. Rev. Lett. **99**, 260401 (2007).
[10] D. M. Whittaker, Phys. Status Solidi C **2**, 733 (2005).
[11] F. M. Marchetti, M. H. Szymańska, C. Tejedor, and D. M. Whittaker, Phys. Rev. Lett. **105**, 063902 (2010).
[12] D. Whittaker, Superlattices Microstruct. **41**, 297 (2007).
[13] G. Tosi *et al.*, J. Phys. Conf. Ser. **210**, 012023 (2010).
[14] L. P. Pitaevskii and S. Stringari, *Bose-Einstein Condensation* (Clarendon Press, Oxford, 2003).
[15] V. Boyer *et al.*, Phys. Rev. Lett. **99**, 143601 (2007).
[16] A. M. Marino *et al.*, Phys. Rev. Lett. **101**, 093602 (2008).
[17] J. J. García-Ripoll *et al.*, Phys. Rev. Lett. **87**, 140403 (2001).